Modelling vegetation understory cover using LiDAR metrics.

Lisa A. Venier[1*], Tom Swystun[1], Marc J. Mazerolle[2], David P. Kreutzweiser[1], Kerrie L. Wainio-Keizer[1], Ken A. McIlwrick[1], Murray E. Woods[3], Xianli Wang[1]

[1] Great Lakes Forestry Centre, Canadian Forest Service, Natural Resources Canada, Saul Ste. Marie, ON, Canada

[2] Department of Biology, Laval University, Quebec, QC, Canada

[3] Ontario Ministry of Natural Resources and Forestry, North Bay, ON, Canada

*Corresponding Author
E-mail: lisa.venier@canada.ca

Abstract

Forest understory vegetation is an important feature of wildlife habitat among other things. Predicting and mapping understory is a critical need for forest management and conservation planning, but it has proved difficult. LiDAR has the potential to generate remotely sensed forest understory structure data, yet this potential has to be fully validated. Our objective was to examine the capacity of LiDAR point cloud data to predict forest understory cover. We modeled ground-based observations of understory structure in three vertical strata (0.5 m to < 1.5 m, 1.5 m to < 2.5 m, 2.5 m to < 3.5 m) as a function of a variety of LiDAR metrics using both mixed-effects and Random Forest models. We compared four understory LiDAR metrics designed to control for the spatial heterogeneity of sampling density. The four metrics were highly correlated and they all produced high values of variance explained in mixed-effects models. The top-ranked model used a voxel-based understory metric along with vertical stratum (Akaike weight = 1, explained variance = 87%, SMAPE=15.6%). We found evidence of occlusion of LiDAR pulses in the lowest stratum but no evidence that the occlusion influenced the predictability of understory structure. The Random Forest model results were consistent with those of the mixed-effects models, in that all four understory LiDAR metrics were identified as important, along with vertical stratum. The Random Forest model explained 74.4% of the variance, but had a lower cross-validation error of 12.9%. Based on these results, we conclude that the best approach to predict understory structure is using the mixed-effects model with the voxel-based understory LiDAR metric along with vertical stratum, but that other understory LiDAR metrics (fractional cover, normalized cover and leaf area density) would still be effective in mixed-effects and Random Forest modelling approaches.

Introduction

Understory vegetation is an important part of the forested ecosystem. It contributes greatly to nutrient cycling (1, 2), wildlife habitat (3-5), fire behaviour (6-8), microclimate (2) and carbon accounting (9). Understory vegetation communities are therefore often considered a good indicator of forest ecological integrity (10, 11) . However, spatial predictions of understory cover or density have been extremely difficult to generate using traditional variables such as topography, overstory and soils (12). Active remote-sensing technology such as LiDAR (light detection and ranging) could potentially address this issue.

LiDAR provides an estimate of three-dimensional forest structure including estimates of canopy structure, understory vegetation and terrain. LiDAR is a survey method that measures the distance to a target (in this case, vegetation) by illuminating the vegetation with a laser light pulse, and measuring the reflected pulses with a sensor. These reflected pulses are called LiDAR returns. Three-dimensional representations of the forest are constructed using laser pulse return times. This capacity has conferred large advantages to forest managers, conservationists and researchers in their attempts to manage the forest efficiently and sustainably. LiDAR can generate reliable, robust estimates of many forest structure variables including canopy height and cover (13-15), as well as basal area and tree density (13, 16) and has similar potential for understory structure.

To date, relatively few studies have evaluated the potential of LiDAR to describe understory structure by comparing ground-based measures of understory structure and LiDAR data (17-20). In each study, different LiDAR metrics were used with a variety of covariates, analytical approaches, and forest types to test predictions of understory cover or density. There

67 is a large discrepancy in the success of the various LiDAR metrics in producing reliable
68 predictions of understory. Our objective in this paper is to evaluate the potential of LiDAR to
69 generate predictions of understory cover by comparing to field measures of understory. To
70 achieve this objective, we examine alternative LiDAR metrics that control for spatial
71 heterogeneity of sampling density, we compare regression and machine learning statistical
72 approaches, and we examine the value of multiple variables in our models.

73 A key challenge of working with LiDAR data is that there is a large amount of spatial
74 heterogeneity in the sampling density over space that occurs in the normal course of
75 generating LiDAR point clouds. This spatial heterogeneity is due to variations in scan angle,
76 flight height, movement of the aircraft during data collection and the degree of overlapping
77 flight lines. Thus, relative measures of vegetation density or cover, where the number of
78 returns in a vertical stratum are scaled relative to some measure of sampling density, should
79 provide better estimates of true understory vegetation cover. A variety of approaches have
80 been used to relativize these measures, for example, dividing the number of returns in a
81 vertical bin by the total number of returns in the column, or by the number of returns in the bin
82 and below the bin (20). We examine four different understory structure metrics based on
83 different approaches to control for sampling density.

84 We explored two statistical approaches for modelling understory vegetation structure
85 as a function of LiDAR data: machine learning and mixed effects regression models. Machine
86 learning, specifically random forest, has been used to model forest inventory variables with a
87 large suite of LiDAR derived predictors (18, 21). Machine learning in this context strives to
88 produce the best prediction of the forest inventory variables. However, machine learning does

not produce an ecologically interpretable relationship per se, only estimates of variable importance. Machine learning makes no assumptions about the structure of the data, is ideal for predicting relationships that are non-linear, is insensitive to correlations among variables, and interactions are automatically modeled. However, machine learning is prone to bias associated with incomplete ranges of conditions being sampled. As an alternative, we explored linear mixed-effects regression models. These models make assumptions of homoscedasticity and normality of errors which must be checked but can produce more parsimonious and more interpretable models than machine learning in some instances. In random forest models, large suites of variables are usually included to achieve the best predictive capacity. In the regression models, it is more important to limit the number of variables included to avoid overfitting and strong correlations between explanatory variables.

Occlusion has been discussed in the literature as a possible issue limiting LiDAR effectiveness for prediction of understory structure (22, 23), but more recent studies have shown that the potential occlusion may not interfere with generating predictions. Latifi et al. (18) demonstrated that artificially reducing the density of the LiDAR point cloud did not have an appreciable effect on variance explained in models predicting understory structure. In another study, prediction errors of understory vegetation cover were not related with canopy cover (17). However, forest type in some instances can influence the predictive accuracy of models (19). In both of our modelling approaches, we included additional variables beyond the understory LiDAR metrics that may influence the amount of occlusion of the laser pulse, namely, the amount of overstory, the forest type, and the vertical stratum. All three of these

variables could reflect the amount of vegetation in the area above the vertical stratum of interest.

Our primary objective is to quantify the capacity of LiDAR to estimate understory structure. To achieve this, 1; we compare the effectiveness of four possible understory LiDAR metrics for predicting understory cover that control for sampling density, 2; we examine the influence of potentially important additional explanatory variables on the model which will inform us about the importance of occlusion, and 3; we compare the mixed effects vs random forest approach for generating predictions. Our aim is to generate robust and effective predictions of understory cover that could inform forest management and conservation.

Methods

Study area

This project was conducted in the Petawawa Research Forest. The research forest covers 9,945 hectares in the Great Lakes-St. Lawrence forest region (45° 58' 46.74" N, 77° 30' 22.11" W), Ontario, Canada. The study area is on the Southern end of the Precambrian Shield, on bedrock of granites and gneisses. Forest composition features White Pine (*Pinus strobus* Linnaeus), Red Pine *(Pinus resinosa* Aiton), Red Oak *(Quercus rubra* Linnaeus), Yellow Birch (*Betula alleghaniensis* Britton), Sugar Maple *(Acer saccharum* Marshall), and Red Maple *(Acer rubrum* Linnaeus) as dominant species, often in uneven-aged forests. Presently, the Petawawa Research Forest is dominated by healthy but mature and overmature overstory (80-140 years)

coupled primarily with low-quality regeneration and understories. For the purpose of the current study, we classified the forest into four types (TYPE) to explore the influence of forest type on the consistency of the relationship between field measured understory vegetation structure and LIDAR metrics. The four forest type classes (TYPE) are Pine, Red Oak, Mixedwood without Pine, and Mixedwood with Pine. These four classes account for approximately 71% of the landbase of the research forest.

Field data collection

Within the Petawawa Research Forest, plots were selected from a 25 m-resolution rasterized LiDAR database and Forest Resource Inventory data based on aerial photo interpretation. Potential plots were selected based on a stratification by forest type, overstory density and understory density. Initial overstory was measured as the relative number of LiDAR laser pulse returns in overstory (> 4 m), and understory density as the relative number of LiDAR laser pulse returns 4 m or lower. We divided the full range of overstory values into 10 equal bins, and the full range of understory values into 10 equal bins. For each combination of understory by overstory bin we selected five potential plots for each of four forest types, for a total of 2000 plots, 500 in each 10 by 10 matrix, with one matrix per each forest type. This is a rough stratification but helped to fill the statistical space to ensure optimal conditions for model construction. We sampled 437 plots out of the possible 2000, trying to select 1-5 plots from all cells in the matrix.

We collected vegetation data on 250 plots in 2015 and on an additional 187 plots in 2016. Plots were selected in the field from the list of preselected plots based on accessibility

and conformity with classified forest type, understory and overstory. At each plot centre, we used an SX Blue II GPS to generate a sub-meter accurate location through averaging a minimum number of 300 points. Our field data collection attempted to generate a field-based point cloud to match the LiDAR based point cloud. We measured forest structure on ground-based plots in nine vertical strata (0-0.5 m, 0.5-1 m, 1-1.5 m, 1.5-2 m, 2-2.5 m, 2.5-3 m, 3-3.5 m, 3.5-4.0 m, > 4 m). From the centre point we created eight radial transects (12 m in length each) starting in a north direction and moving clockwise by 45 degrees for each additional transect. Along each transect, data were collected at each meter for a total of 97 sample locations in each plot, including the centre point (Fig 1). To sample the vegetation structure, observers recorded the presence or absence of vegetation within a 15 cm circle for each of the nine vertical strata. Thus, there were 97 sampling points x 9 strata = 873 presence/absence points collected in each 12 m radius plot volume. The original vertical strata were later grouped into three strata (S1 = 0.5-1.5 m, S2 = 1.5-2.5 m, S3 = 2.5-3.5 m). We excluded points below 0.5 as they are difficult to distinguish from ground points. We excluded points above 3.5m as they were difficult to estimate from the ground. The total number of vegetation presences in each stratum (0-194) were recorded in the FIELD variable for subsequent analysis. This field collection would represent a lower sampling density than the LiDAR data which are at 6 pulses per square meter with up to 8 returns per pulse which resulted in 2.44 returns per m^3 compared to the field data with 0.43 returns per m^3. These data are not strictly comparable since the field data represent presence and absence whereas the LiDAR returns represent only presence but give a general impression of relative sampling density.

Fig 1. Sampling design for FIELD observations of vegetation structure. r is the radius of the measurement area around each point on the transect.

LiDAR acquisition

Airborne LiDAR data were collected over the Petawawa Research Forest from August 17-20, 2012. The Riegl 680i sensor was carried aboard a Cessna 172 aircraft flown at an average altitude of 750 m. Technical acquisition specifications are provided in Table 1. The data were collected as a full-waveform and provided as a discrete point file (LAS 1.1) for use in this project. Flight overlap was approximately fifty percent.

Table 1. Airborne LiDAR acquisition specifications.

Parameter	Value
Pulse repetition rate	150Khz
Frequency	76.67Hz
Scan Angle	± 20 Degrees
FOV	40 Degrees
Line spacing: Cross track	0.6 m
Line spacing: Along track	0.6 m
Line spacing between flight lines	250 m
Laser footprint min:	0.38 m
Laser footprint max	0.42 m
Average point density: All Returns	~ 15 pts/m^2
Average point density: Last Returns	~ 6 pts/m^2

Data processing and LiDAR variables

We developed specific LiDAR understory cover metrics that are expected to capture the vegetation understory density directly. We identified four metrics for our analysis. Three of these metrics are used in the literature: fractional cover (FRAC, modified from Wing et al. (17)), leaf area density (LAD, (24)), and voxel cover (VOX1m, (25)). The fourth metric considered was

194 normalized cover (NORM), because it is an easily interpretable and easily calculated alternative.
195 Fractional cover is calculated by summing the number of LiDAR vegetation returns for each
196 understory vertical stratum and dividing by the sum of understory and ground returns. Leaf
197 area density is calculated as the negative log of the number of returns in a vertical stratum
198 divided by all returns in and below the vertical bin and then divided by a constant. Normalized
199 cover is calculated by dividing all vegetation returns in the understory stratum divided by all
200 first returns. The voxel cover approach filters all returns by estimating presence/absence of
201 returns in each standard voxel (in our case 1 m^3) in the vertical stratum. For example, a 2 m x 5
202 m x 5 m vegetation stratum that contains 50 1-m^3 voxels would have a voxel cover value
203 between 0 and 50, equal to the number of voxels that contain vegetation. Sampling density is
204 extremely heterogeneous due to different factors such as flight line overlap and the pitch and
205 yaw of the plane. The LiDAR metrics provide four alternative ways to scale the number of
206 returns in a vertical bin by sampling density. In addition to these four specific LiDAR understory
207 cover metrics, we calculated a suite of standard LiDAR point cloud metrics such as canopy cover
208 and canopy height (S1 Table).
209

210 ## Analysis

211 We used linear mixed effects models to determine the capacity of our four main LiDAR
212 understory cover metrics to predict understory cover recorded in the field (FIELD) in each of the
213 three vertical strata defined above (ST1, ST2, ST3), and to examine the influence of secondary
214 explanatory variables(26). These secondary explanatory variables consisted of forest TYPE
215 (based on overstory composition), STRATUM (vertical 1 m strata, ST1-ST3), and OVERSTORY

(Appendix 1). The OVERSTORY variable was a measure of LiDAR vegetation cover in the vertical column above the stratum of interest calculated by classifying canopy cover (CC) into three classes (low, medium, high). We treated the plot as a random effect to account for multiple measurements in each plot. We formulated 16 candidate models consisting of LiDAR variables, with the constraint of maintaining variance inflation factors (VIF) < 10 to avoid issues of multicollinearity (Table 2). For each the four main LiDAR metric, we derived four models: 1) a null model consisting only the LiDAR metric, 2) a model with the LiDAR metric, OVERSTORY and their interaction, 3) a model with the LiDAR metric, TYPE, and their interaction, and 4) a model with the LiDAR metric, STRATUM, and their interactionWe ranked all mixed effects models based on Akaike's information criterion (AIC, (27, 28)) and calculated the R^2 values. We also computed the symmetric mean absolute percentage error (SMAPE), based on 10-fold cross-validation (29) for the top-ranked models, and calculated SMAPE values for each of the 3 vertical strata separately. Parameters of the mixed effects models were estimated by maximum likelihood in R with the nlme package(18, 26, 30).

Table 2: Mixed effects model explaining understory cover recorded in the field (FIELD) : TYPE = forest type based on overstory composition, STRATUM = vertical 1 m strata, S1-S3, and OVERSTORY = a measure of LiDAR vegetation cover in the vertical column above the stratum of interest calculated by classifying canopy cover (CC) into three classes (low, medium, high), see Appendix 1. The plot was treated as a random effect in each model.

Model Name	Model fixed effects structure	Biological interpretation
FRAC null	FRAC	Relationship between FRAC and FIELD is constant
FRAC * STRATUM	FRAC + STRATUM + FRAC*STRATUM	Relationship between FRAC and FIELD differs among STRATUM
FRAC * OVERSTORY	FRAC + OVERSTORY + FRAC*OVERSTORY	Relationship between FRAC and FIELD differs among OVERSTORY

FRAC * TYPE	FRAC + TYPE + FRAC*TYPE	Relationship between FRAC and FIELD differs among TYPE
NORM null	NORM	Relationship between NORM and FIELD is constant
NORM * STRATUM	NORM + STRATUM + NORM*STRATUM	Relationship between NORM and FIELD differs among STRATUM
NORM * OVERSTORY	NORM + OVERSTORY + FRAC*OVERSTORY	Relationship between NORM and FIELD differs among OVERSTORY
NORM * TYPE	NORM + TYPE + FRAC*TYPE	Relationship between NORM and FIELD differs among TYPE
VOX1m null	VOX1m	Relationship between VOX1m and FIELD is constant
VOX1m * STRATUM	VOX1m +STRATUM + VOX1m*STRATUM	Relationship between VOX1m and FIELD differs among STRATUM
VOX1m * OVERSTORY	VOX1m + OVERSTORY + VOX1m*OVERSTORY	Relationship between VOX1m and FIELD differs among OVERSTORY
VOX1m * TYPE	VOX1m + TYPE + VOX1m*TYPE	Relationship between VOX1m and FIELD differs among TYPE
LAD (null)	LAD	Relationship between LAD and FIELD is constant
LAD * STRATUM	LAD + STRATUM + LAD*STRATUM	Relationship between LAD and FIELD differs among STRATUM
LAD * OVERSTORY	LAD + OVERSTORY + LAD*OVERSTORY	Relationship between LAD and FIELD differs among OVERSTORY
LAD * TYPE	LAD + TYPE + LAD*TYPE	Relationship between LAD and FIELD differs among TYPE

We used random forest with the same FIELD response variable as in the mixed-effects models described above. Because random forests are non-parametric and do not yield a log-likelihood, we ran a stepwise procedure with 341 LiDAR derived variables (which includes overstory estimates) (S1 Table), plus secondary variables forest TYPE (from Forest Resource Inventory), and STRATUM. We used mean decrease in accuracy to rank variable importance (31). At each iteration, we removed the 20% least influential variables and compared the explained variance. Models were built using the randomForest package in R (31). We examined the importance of variables in the suite of random forest models. Similar to the mixed effects models above, we quantified model performance with the percent variance explained and SMAPE based on 10-fold cross-validation. Finally, we compared the prediction performance of the mixed effects and random forest approaches.

Results

Relationship among LiDAR metrics

The FIELD measure of understory cover was strongly correlated with all of the four main LiDAR metrics we investigated (Fig 2a-d). However, the FRAC and VOX1m metrics appeared to be the most linearly related to the FIELD measure (Fig 2a-d). Nonetheless, the four understory vegetation metrics were all highly correlated with one another (Table 3).

Fig 2. Scatterplot of FIELD (measured density) against the LiDAR metrics, a) fractional cover (FRAC), b) normalized cover (NORM), c) leaf area density (LAD), and d) voxel cover (VOX1m), including Pearson product-moment correlation coefficients.

Table 3. Pearson product-moment correlations between pairs of understory cover LiDAR metrics included in analysis (n = 1310).

Correlation	r	Lower 95% CL	Upper 95% CL
FRAC vs NORM	0.77	0.751	0.794
FRAC vs VOX1m	0.84	0.819	0.852
FRAC vs LAD	0.77	0.744	0.789
NORM vs LAD	0.81	0.79	0.827
NORM vs VOX1m	0.92	0.911	0.927
VOX1m vs LAD	0.79	0.767	0.808

Mixed-effects models

The model consisting of the voxel-based cover estimate (VOX1m) with STRATUM and their interaction was the most parsimonious among all sixteen models considered (Table 4). This model had all the support (Akaike weight = 1, Table 4, Fig 3). This model also had the highest conditional R^2 (along with the FRAC + STRATUM + interaction model, although all sixteen models had high R^2 values (0.71-0.87). For each the four LiDAR metrics we considered, we observed the same pattern: the addition of STRATUM and the interaction to the null models resulted in consistently better model performance in terms of delta AIC and R^2. The addition of OVERSTORY or TYPE resulted in much less model improvement than the addition of STRATUM. The model with most support did not include forest type or overstory, which is important since forest type was derived from forest inventory data and cannot be extracted from LiDAR point clouds.

Table 4. R^2 and AIC values for sixteen candidate linear mixed-effects models. Note that marginal R^2 denotes the percent variance explained by the fixed effects, whereas the conditional R^2 includes both fixed effects and random effects. Delta AIC is the difference

283 between each model relative to the most parsimonious model and Akaike weight indicates the
284 percent support of a given model. .
285

Model	Marginal R^2	Conditional R^2	AIC	Delta AIC	Akaike weight
VOX1m * STRATUM	0.62	0.87	11868.87	0	1
FRAC * STRATUM	0.65	0.87	11901.00	32.13	0
LAD * STRATUM	0.56	0.82	11998.29	129.42	0
NORM * STRATUM	0.52	0.83	12099.16	230.29	0
VOX1m * OVERSTORY	0.60	0.82	12348.32	479.45	0
LAD * OVERSTORY	0.51	0.73	12384.88	516.01	0
VOX1m * TYPE	0.60	0.82	12384.88	516.01	0
VOX1m null	0.60	0.82	12385.78	516.91	0
LAD * TYPE	0.51	0.72	12396.42	527.55	0
LAD null	0.50	0.71	12407.11	538.24	0
NORM * OVERSTORY	0.53	0.75	12450.66	581.79	0
NORM * TYPE	0.51	0.75	12563.97	695.1	0
NORM null	0.49	0.75	12568.4	699.53	0
FRAC * OVERSTORY	0.58	0.77	12585.04	716.17	0
FRAC * TYPE	0.57	0.75	12613.19	744.32	0
FRAC null	0.56	0.75	12617.05	748.18	0

286

287 **Figure 3: Predicted versus observed scatterplot.** Predictions of FIELD generated from mixed-
288 effects model consisting of VOX1m + STRATUM + interaction.
289

290 In all of the mixed effects models, the four LiDAR metrics had positive slopes (Fig 4,
291 Table 5, for example). In our best model, the intercept of the lowest STRATUM was higher than
292 in the upper strata (Fig 4). Although the model included the interaction between STRATUM and
293 voxel cover, there was no evidence of different slopes of LiDAR among strata (Fig 4, Table 5).
294 Symmetric mean absolute percentage (SMAPE) errors for the top-ranked mixed effects model
295 was 0.156, but these values varied when investigating each stratum separately (Table 6).
296 Contrary to expectations, the SMAPE value was lowest for the lowest strata (0.107) and
297 greatest for the highest strata (0.190). There were 437 observations for each stratum.

Figure 4: Predictions of FIELD for each of three strata based on the mixed-effects model consisting of VOX1m + STRATUM + interaction. Dashed lines around solid lines denote 95% confidence intervals around predictions.

Table 5. Estimates of the best supported mixed-effects model consisting of VOX1m + STRATUM + interaction and a random effect of plot.

	Estimate	Lower 95% CL	Upper 95% CL
intercept	64.35	60.25	68.46
LIDAR	0.03	0.29	0.32
STRATUM.ST2	-21.94	-25.96	-17.98
STRATUM.ST3	-29.38	-33.48	-25.28
LIDAR*STRATUM.ST2	-0.016	-0.039	0.008
LIDAR*STRATUM.ST3	-0.010	-0.037	0.017

Table 6. Ten-fold cross-validation results from top linear mixed-effects model and the selected random forest model, based on symmetric mean absolute percentage error (SMAPE). Note that average values of SMAPE are given for predictions of all STRATUM levels, but also for predictions specific to STRATUM levels.

Model		SMAPE mean	SMAPE sd (n=10)
VOX1m * STRATUM	predictions of all STRATUM levels	0.156	0.014
	predictions of STRATUM 1	0.107	0.016
	predictions of STRATUM 2	0.170	0.024
	predictions of STRATUM 3	0.190	0.020
Random forest (59 predictors)		0.129	0.015

Random forest models

We examined the percent variance explained and the number of variables included to choose a final random forest model. The base model with all 341 LiDAR-derived variables, forest TYPE, and STRATUM explained 74.8% of the variance, but the final model with only 59 predictors had a very similar variance explained (74.4%) (Fig 5, Table 7). The 10-fold cross-validation on this reduced model showed an overall mean error rate of 0.129 (Table 6).

Fig 5. Predicted versus observed scatterplot for Random Forest model with 59 predictors.

Some variables appeared more often than others among the 18 random forest models considered. These variables consisted of STRATUM, GAP (the inverse of LAD), and LAD. In addition, most or all of the LiDAR understory vegetation cover metrics (VOX1m, FRAC, NORM) were represented in the top 10 variables of most of the 18 potential models (S2 Table). Crown closure (CC), an estimate of overstory, was also often among the top 10 most important variables within the models considered. Forest TYPE never occurred among the top 10 variables (S2 Table).

Table 7. Random forest models: mean squared residuals and percent variance explained.

Number of Predictors in model	Mean Squared Residuals	Percent variance Explained
341 (Base model)	484	74.8
276	485	74.7
223	485	74.8
180	484	74.7
145	476	75.2
116	486	74.7
93	481	75.0

74	492	74.3
59	490	74.4
47	513	73.3
37	508	73.5
29	531	72.4
22	553	71.2
17	528	72.5
13	558	70.9
10	580	69.8
7	569	70.4
5	632	67.1

Discussion

In this study, our primary objective was to quantify the capacity of LiDAR to estimate understory structure so that it can be predicted across a landscape. To address this objective, first we compared the effectiveness of four possible understory LiDAR metrics (fractional cover, leaf area density, voxel cover, and normalized cover) for predicting understory cover. Each of these metrics used some measure of the number or presence of LiDAR returns in an understory vertical stratum and standardized these measures with an estimate of sampling density. All four LiDAR metrics were effective at predicting the amount of structure in an understory stratum, but the best metric based on mixed effects modelling was the voxel-based cover estimate (VOX1m) with the addition of STRATUM with a conditional R^2 of 0.87. The voxel-based approach is relatively easy to calculate and provides a direct measure of the amount of understory structure.

We anticipated that other variables could influence the predictions of understory. We identified three potentially important variables that might influence occlusion of understory structure: overstory, forest type and stratum. Increased overstory can reduce the ability of

LiDAR to predict understory structure due to occlusion (22, 23). For LiDAR to detect the understory structure, LiDAR pulses must reach and be reflected by understory vegetation. A greater vegetation interception above the area of interest will result in fewer pulses returning from the understory. Both forest type and stratum will also influence the amount of vegetation in the area above the area of interest and therefore potentially alter the relationship of field measured and LiDAR measured understory.

Correlations between the three secondary explanatory variables (STRATUM, forest TYPE, and OVERSTORY) made it impossible to include all variables in a single model. Our best model included STRATUM, where we found that the lowest stratum had the highest intercept. This is consistent with occlusion in that we have more vegetation in ST1 than ST2 and ST3 for a given value of VOX1m. This is consistent with the idea that fewer laser pulses are reaching the lower stratum. The relationship between the field observed structure and VOX1m did not vary with STRATUM. Surprisingly, we found that the error in the predicted relationship was greatest in the highest STRATUM and lowest in the lowest STRATUM suggesting that there was no reduction in predictability associated with potential occlusion. This may be due to the possibility that the understory vegetation in the lower stratum is easier to estimate on the ground and therefore there is less noise in the relationship between the field and the LiDAR measures in the lower stratum. Either way, we conclude that our LiDAR sampling intensity was sufficient in our forest system to capture the understory structure regardless of the density of vegetation above the area of interest and the related potential for occlusion.

There is some discrepancy in the literature on the effect of occlusion. Latifi et al. (19) found that thinning LiDAR data by artificially reducing the sampling density did not impact the effectiveness of models to predict understory. Their original data had a high point density of 30-40 points per m^2 and a maximum of 11 returns. Data were thinned to two different levels but Latifi et al. (19) do not report on the final point density after thinning. Our data are at roughly 11.69 vegetation returns per m^2, with about 0.55 vegetation returns per m^3 in the 0.5-4m understory stratum. Obviously, the effectiveness of LiDAR to capture understory structure will eventually be undermined by a sufficient reduction in sampling density, but this limit does not seem to have been reached in the Petawawa research forest. Gonzalez-Ferreiro et al. (32) showed that reducing pulse density from 8 pulses per m^2 to 0.5 pulses per m^2, did not decrease model precision in estimating stand variables. Wing et al. (17) found no trends between understory vegetation cover prediction error and canopy cover, lending support to the idea that under some natural overstory conditions and common LiDAR sampling densities, occlusion is not an issue for predicting understory with LiDAR. In contrast, Ruiz et al. (33) reported an effect of LiDAR sampling density on model R^2 values but only at levels below around 5 points/m^2. It is unclear how this number translates into pulses reaching the understory. The lack of influence of forest type on understory cover predictions enables predicting understory from LiDAR alone without relying on traditional forest resource inventory data.

The comparisons of mixed effects and random forest models revealed some obvious alignment. All four of the LiDAR metrics considered (fractional cover, leaf area density, normalized cover, and voxel cover) produced models with high R^2 values. All four of these variables also had very high variable importance in the random forest models. The stratum

variable appeared often in the top random forest models and was also important in the top-ranked mixed-effects model (VOX1m * STRATUM). The random forest model had a high variance explained (75%), but not as high as the best mixed effects model that included the voxel-based measure of cover (87%). Our selected random forest model had 59 explanatory variables, whereas the best mixed effects model had two explanatory variables and their interaction, as well as a random effect of plot. Based on our results, generating landscape-wide predictions using the mixed-effects model should be simpler and more efficient than with the random forest model. For these reasons, although the random forest model is effective, we recommend the mixed effects model as the better choice for predicting understory vegetation structure with LiDAR.

Direct evaluations of LiDAR metrics to capture understory cover are relatively rare. Studies have shown good agreement between field and LiDAR measures of forest stand biomass (34, 35), but biomass is likely driven primarily by tree biomass rather than understory. Asner et al. (36) explored structural transformation of rain forests due to invasive plants and used LiDAR to estimate structural changes in the understory. However, Asner et al. (36) did not report quantitative comparisons of field and LiDAR measures. Martinuzzi et al. (37) produced classification accuracies of 83% in predicting the presence of shrubs, but not their abundance. Wing et al. (17) compared understory vegetation cover and airborne LiDAR estimates with the addition of a filter for intensity values in an interior ponderosa pine forest. Their models had R^2 values from 0.7 to 0.8 and accuracies of ± 22%. Our models achieved slightly higher R^2 with slightly lower error rates without the use of the intensity filter, suggesting that the latter filter may not always be necessary to generate good estimates. As well, the intensity filter is affected

by a number of factors such as elevation and the nature of the object intercepted that are difficult to normalize, so we prefer models that do not require intensity filters. Latifi et al. (19) also made a direct comparison of ground-based vs LiDAR estimates of understory cover in temperate mixed stands, and found strong relationships in the top canopy and the herbal layer with lower predictive power in the intermediate stand layers. Their shrub layer regression model had a relatively low R^2 value of 37%. In a later study, Latifi et al. (18) showed an R^2 of 80% for the shrub layer based on thinned LiDAR point clouds and new analytical methods. Campbell et al. (20) also compared field and LiDAR measures of understory directly in mixedwood forests and generated an R^2 of 0.44 based on a relative point density similar to metrics that we used here. It is unclear why there is so much variation in the ability of LiDAR to predict understory structure but it suggests that we should be somewhat cautious in assuming that individual LiDAR metrics are capturing the understory structure. It is important to note that some of the error in prediction in our models is likely the result of the lag between the LiDAR acquisition (2012) and the field data acquisition (2016-2017). This lag is likely to result in the most error in the youngest stands where changes in herb and shrub growth are likely to be greatest. The majority of stands included in the analysis are mature forest, and even with this source of error our ability to predict was good.

Despite the limited work directly evaluating LiDAR measures of understory vegetation structure, many studies have explored the use of LiDAR to capture wildlife habitat structure some of which is related to understory (38-42). One of the most commonly reported relationships is between vegetation structural diversity or understory density and wildlife diversity (5, 43-45). In addition, vegetation understory structure explained bird species

437 composition in a number of studies (5, 46, 47). Melin et al. (48) found that a LiDAR metric
438 similar to fractional cover to estimate shrub density below 5 m was a good predictor of grouse
439 brood occurrence in Finland, consistent with expectations based on known habitat preferences
440 of the species. However, they did not test the assumption that the LiDAR metric effectively
441 estimates vegetation density below 5 m. All of these studies do however, provide indirect
442 evidence for the effectiveness of LiDAR estimates to predict understory cover or density.
443

444 # Conclusions

445 Based on the highest variance explained, the fewest number of explanatory variables,
446 and ease of interpretation and application, we would recommend using the mixed-effects
447 model consisting of voxel-based cover estimate, stratum, and their interaction to generate
448 spatial estimates of understory cover. Nonetheless, all four LiDAR metrics that we considered
449 and both analytical approaches (mixed effects models, random forests) produced predictions
450 suitable for many ecological and forest planning applications. This information could improve
451 spatially-explicit mapping of wildlife habitat, fire behaviour, or forest ecosystem dynamics.
452 Measuring understory cover *in situ* is not difficult, but many applications require maps or
453 spatial estimates of attributes for forest management and conservation applications over large
454 areas. LiDAR remote sensing is the most efficient approach to generating these spatial
455 estimates of forest attributes. Our results fully support the indirect evidence provided from
456 wildlife studies that LiDAR can predict understory vegetation structure even in the presence of
457 a mature tree canopy. With error percentages of around 15%, these spatial predictions will
458 introduce some uncertainty into predictions, which should be factored into decision-making.

459

460 # Acknowledgements

461 Nicholas Coops and Piotr Tompalski provided guidance and training on LiDAR data

462 handling. Peter Arbour and staff at the Petawawa Research Forest provided logistic support.

463

464 # References

465 1. Yarie J. The role of understory vegetation in the nutrient cycle of forested ecosystems in
466 Mountain Hemlock Biogeoclimatic Zone. Ecology. 1980;61:1498-514.
467 2. Nilsson M-C, D.A. W. Understory vegetation as a forest ecosystem driver: evidence from the
468 Northern Swedish boreal forest. Front Ecol Environ. 2005;3:421-8.
469 3. MacArthur RH, MacArthur JW. On bird species diversity. Ecology. 1961;42:594-8.
470 4. Venier LA, Pearce JL. Boreal forest landbirds in relation to forest composition, structure, and
471 landscape: Implications for forest management. Can J For Res. 2007;37(7):1214-26.
472 5. Lesak AA, Radeloff VC, Hawbaker TJ, Pidgeon AM, Gobakken T, Contrucci K. Modeling forest
473 songbird species richness using LiDAR-derived measures of forest structure. Remote Sens Environ.
474 2011;115:2823-35.
475 6. Bessie WC, Johnson EA. The relative importance of fuels and weather on fire behavior in
476 subalpine forests. Ecology. 1995;76:747-62.
477 7. Call PT, Albini FA. Aerial and surface fuel consumption in crown fires. Int J Wildland Fire.
478 1997;7:259-64.
479 8. Hély C, Bergeron Y, Flannigan MD. Effects of stand composition on fire hazard in mixed-wood
480 Canadian boreal forest. J Veg Sci. 2000;11:813-24.
481 9. Roxburgh SH, Karunaratne SB, Paul KI, Lucas RM, Armston D, Sun J. A revised above-ground
482 maximum biomass layer for the Australian continent. For Ecol Manage. 2019;432:264-75.
483 10. Kerns BK, Ohmann JL. Evaluation and predicition of shrub cover in coastal Oregon forests (USA).
484 Ecol Indic. 2004;4:83-98.
485 11. Suchar VA, Crookston NL. Understory cover and biomass indices predictions for forest
486 ecosystems of Northwestern United States. Ecol Indic. 2010;10:602-9.
487 12. Eskelson BNI, Madsen L, Hagar JC, Temesgen H. Estimating riparian understory vegetation cover
488 with beta regression and copula models. Forest Sci. 2011;57:212-21.
489 13. Lim K, Treitz P, Baldwin K, Morrison I, Green J. LiDAR remote sensing of biophysical properties of
490 tolerant northern hardwood forests. Can J Remote Sens. 2003;29:658-78.
491 14. Naesset E. Practical large-scale forest stand inventory using a small-footprint airborne scanning
492 laser. Scand J Forest Res. 2004;19:164-79.
493 15. Thomas V, Treitz P, McCaughey JH, Morrison I. Mapping stand-level forest biophysical variables
494 for a mixedwood boreal forest using lidar: an examination of scanning density. Can J For Res.
495 2006;36:34-47.
496 16. Woods M, Lim K, Treitz P. Predicting forest stand variables from LiDAR data in the Great Lakes-
497 St. Lawrence Forest of Ontario. Forest Chron. 2008;84:827-39.

17. Wing BM, Ritchie MW, Boston K, Cohen WB, Gitelman A, Olsen MJ. Prediction of understory vegetation cover with airborne LiDAR in an interior ponderosa pine forest. Remote Sens Environ. 2012;124:730-41.
18. Latifi H, Hill S, Schumann B, Heurich M, Dech S. Multi-model estimation of understory shrub, herb and moss cover in temperate forest stands by laser scanner data. Forestry. 2017;90:496-514.
19. Latifi H, Heurich M, Hartig F, Müller J, Krzystek P, Jehl H, et al. Estimating over- and understorey canopy density of temperate mixed stands by airborne LiDAR data. Forestry. 2016;89:69-81.
20. Campbell MJ, Dennison PEH, A., Parham LM, Butler BW. Quantifying understory vegetation density using small-footprint airborne lidar. Remote Sens Environ. 2018;215:330-42.
21. Penner M, Pitt DG, Woods ME. Parametric vs. nonparametric LiDAR models for operational forest inventory in boreal Ontario. Can J Remote Sens. 2013;39(5):426-43.
22. Hill RA, Broughton RK. Mapping the understory of deciduous woodland from leaf-on and leaf-off airborne LiDAR data: a case study in lowland Britain. ISPRS J Photogramm. 2009;64:223-33.
23. Morsdorf F, Marell A, Koetz B, Cassagne N, Pimont F, Rigolot E, et al. Discrimination of vegetation strata in a multi-layered Mediterranean forest ecosystem using height and intensity information derived from airborne laser scanning. Remote Sens Environ. 2010;114:1404-15.
24. Bouvier M, Durrieu S, Rounier RA. Generalizing predictive models of forest inventory attributes usin an area-based approach with airborne LiDAR data. . Remote Sens Environ. 2015;156:322-34.
25. Kim E, Lee W-K, Yoon M, Lee J-Y, Son Y, Abu Salim K. Estimation of Voxel-Based Above-Ground Biomass Using Airborne LiDAR Data in an Intact Tropical Rain Forest, Brunei. Forests. 2016;7(11):259.
26. Pinheiro J, Bates D, DebRoy S, Sarkar D, RCoreTeam. nlme: Linear and Nonlinear Mixed Effects Models. R package version 3.1-137
ed2018.
27. Burnham KP, Anderson DR. Model Selection and Multimodel Inference: a practical information-theoretic approach. 2 ed. New York: Springer-Verlag; 2002.
28. Nakagawa S, Schielzeth H. A general and simple method for obtaining R2 from generalized linear mixed effects models. Methods Ecol Evol. 2013;4:133-42.
29. Gneiting T. Making and evaluating point forecasts. Journal of American Statistical Association. 2011;106:746-62.
30. RCoreTeam. R: A language and environment for statistical computing. . R Foundation for Statistical Computing. Vienna, Austria2018.
31. Liaw A, Wiener M. Classification and regression by randomForest. R News. 2002;2:18-22.
32. Gonzalez-Ferreiro E, Dieguez-Aranda, Miranda D. Estimation of stand variables in Pinus radiata D. Don plantations using different LiDAR pulse densities. Forestry. 2012;85:281-92.
33. Ruiz LA, Hermosilla T, Mauro F, Godino M. Analysis of the influence of plot size and LiDAR density on forest structure attribute estimates. Forests 2014;5:936-51.
34. Hyde P, Dubayah R, Walker W, Blair JB, Hofton M, Hunsaker C. Mapping forest structure for wildlife habitat analysis using multi-sensor (LiDAR, SAR/InSAR, ETM+, Quickbird) synergy. Remote Sens Environ. 2006;102:63-73.
35. Hyde P, Dubayah RP, B., Blair JB, Hofton M, Hunsaker C, Knox R, et al. Mapping forest structure for wildlife habitat analsyis using waveform lidar: validaton of montane ecosystems. Remote Sens Environ. 2005;96:427-37.
36. Asner GP, Hughes RF, Vitousek PM, Knapp DE, Kennedy-Bowdoinm T, Boardmann J, et al. Invasive plants transform the three-dimensional structure of rain forests. PNAS. 2008;105:4519-23.
37. Martinuzzi S, Vierling LA, Gould WA, Falkowski MJ, Evans JS, Hudak AT, et al. Prediction of understory vegetation cover with airborne LiDAR in an interior ponderosa pine forest. Remote Sens Environ. 2009;124:730-41.

545 38. Lefsky MA, Cohen WB, Parker GG, Harding DJ. LiDAR remote sensing for ecosystem studies.
546 BioScience. 2002;52:19-30.
547 39. Bradbury RB, Hill RA, Mason DC, Hinsley SA, Wilson JD, Balzter H, et al. Modelling relationships
548 between birds and vegetation structure using airborne LiDAR data: A review with case studies from
549 agricultural and woodland environments. Ibis. 2005;147(3):443-52.
550 40. Vierling KT, Vierling LA, Gould WA, Martinuzzi S, Clawges RM. Lidar: Shedding new light on
551 habitat characterization and modeling. Front Ecol Environ. 2008;6(2):90-8.
552 41. Davies AB, Asner GP. Advances in animal ecology from 3D-LiDAR ecosystem mapping. Trends in
553 Ecology and Evolution 2014;29:681-91.
554 42. Rechsteiner C, Zellweger F, Gerber A, Breiner FT, Bollmann K. Remotely sensed forest habitat
555 structures improve regional species conservation. Remote Sens Ecol Conserv. 2017;3:247-58.
556 43. Vogeler JC, Hudak AT, Vierling LA, Evans J, Green P, Vierling KT. Terrain and vegetation structural
557 influences on local avian species richness in two mixed-conifer forests. Remote Sens Environ.
558 2014;147:13-22.
559 44. Coops NC, Tompaski P, Nijland W, Rickbeil GJM, Nielsen SE, Bater CW, et al. A forest structure
560 habitat index based on airborne laser scanning. Ecol Indic. 2016;67:346-57.
561 45. Clawges R, Vierling K, Vierling L, Rowell E. The use of airborne lidar to assess avian species
562 diversity, density, and occurrence in a pine/aspen forest. Remote Sens Environ. 2008;112(5):2064-73.
563 46. Müller J, Stadler J, Brandl R. Composition versus physiognomy of vegetation as predictors of bird
564 assemblages: The role of lidar. Remote Sens Environ. 2010;114(3):490-5.
565 47. Vierling LA, Vierling KT, Adam P, Hudak AT. Using satellite and airborne LiDAR to model
566 woodpecker habitat occupancy at the landscape scale. PLoS ONE. 2013;8(12).
567 48. Melin M, Mehtätalo L, Miettinen J, Tossavainen S, Packalen P. Forest structure as a determinant
568 of grouse brood occurrence: an analysis linking LiDAR data with presence/absence field data. For Ecol
569 Manage. 2016;380:202-11.
570

571 Supporting information

572 **S1 Table. Definitions of all variables included in at least one of the mixed-effects or Random**

573 **Forest models.**

574 **S2 Table. Frequency of explanatory variables among the 18 random forest models run with**

575 **341 to 7 variables.**

576 **S3 Data. Data used in analyses for manuscript. Variable definitions are found in S1.**

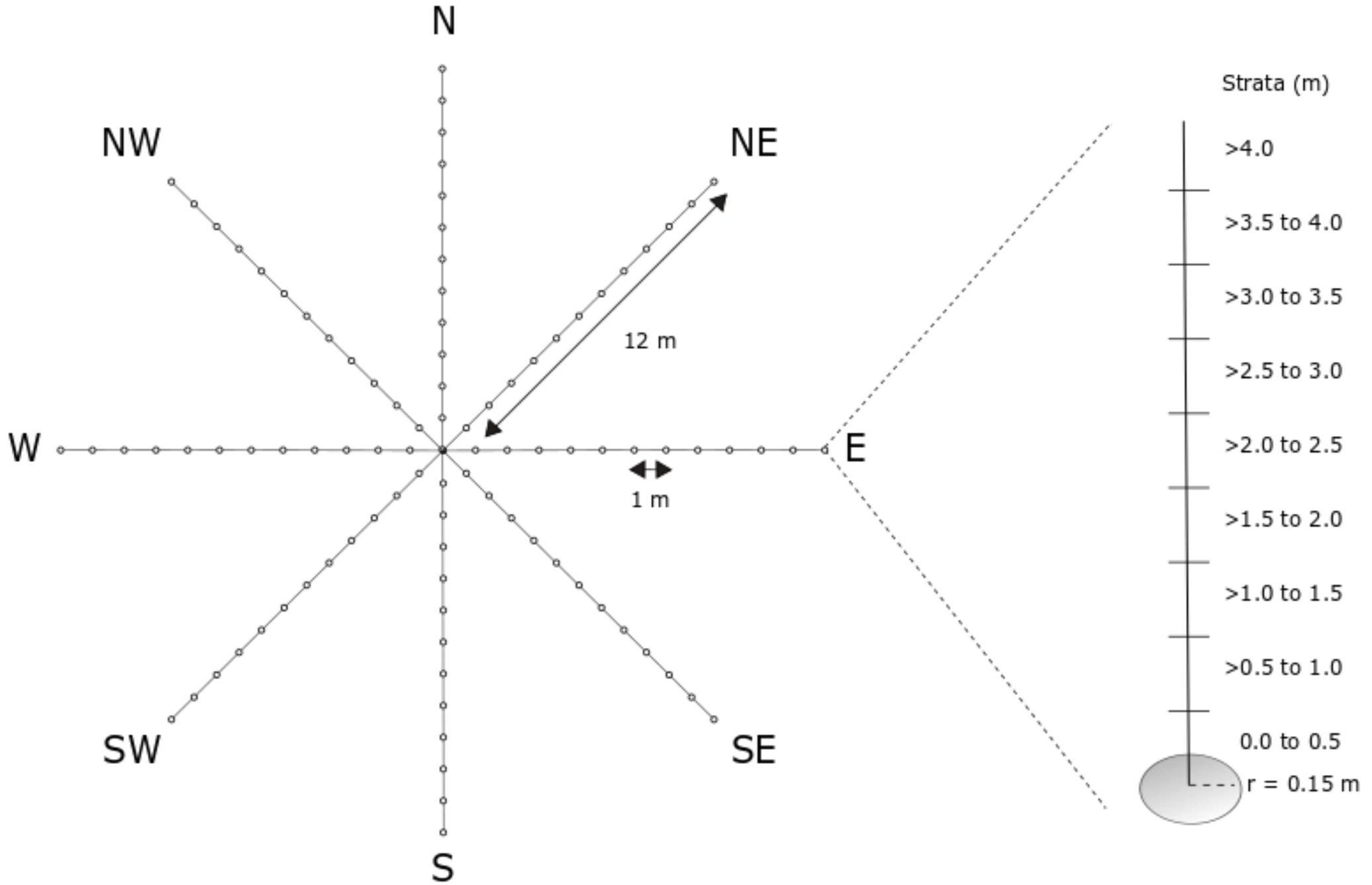
N
NW
NE
W
E
SW
SE
S
12 m
1 m
Strata (m)
>4.0
>3.5 to 4.0
>3.0 to 3.5
>2.5 to 3.0
>2.0 to 2.5
>1.5 to 2.0
>1.0 to 1.5
>0.5 to 1.0
0.0 to 0.5
r = 0.15 m

Figure 1

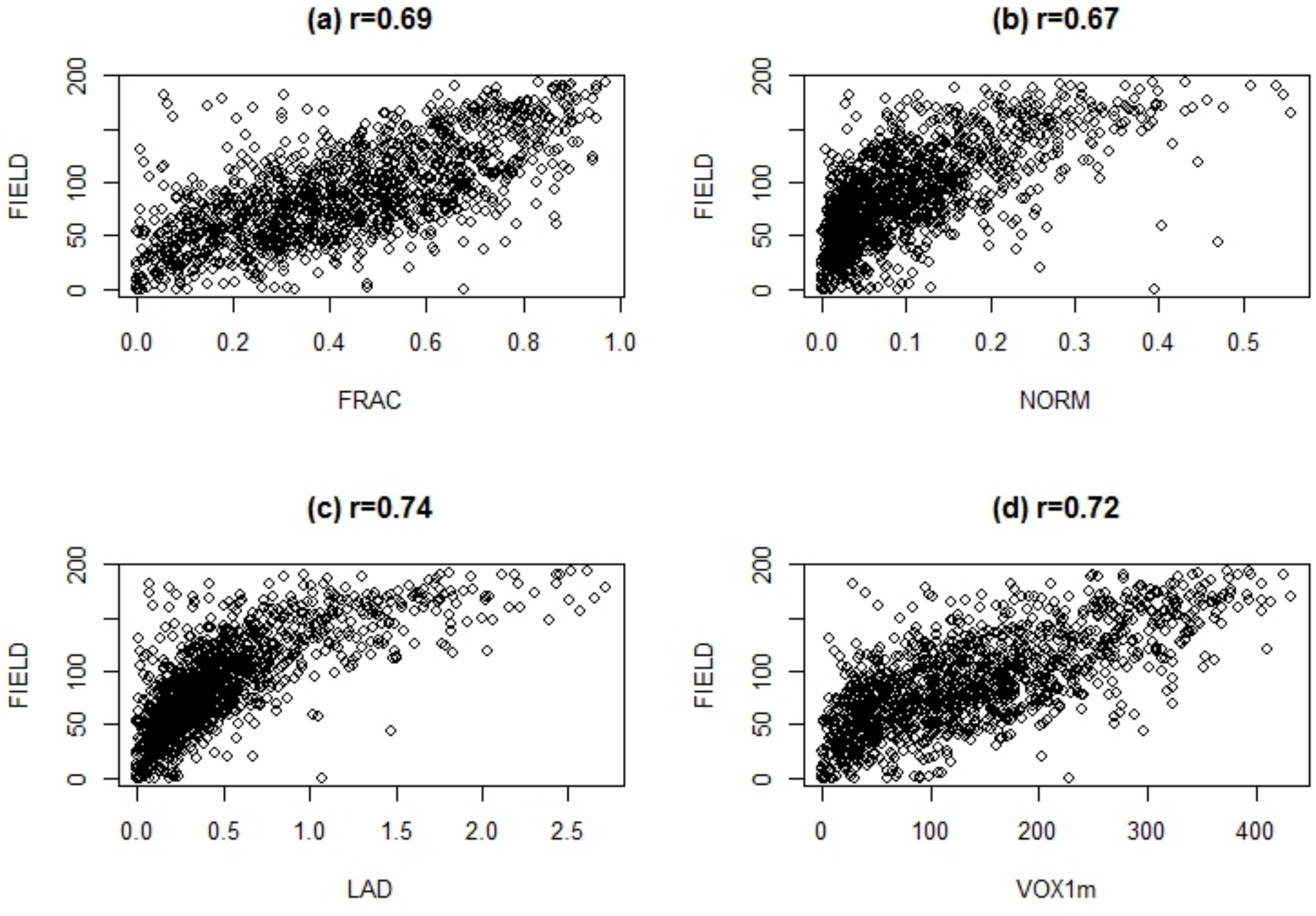
(a) r=0.69
FIELD
FRAC
(b) r=0.67
FIELD
NORM
(c) r=0.74
FIELD
LAD
(d) r=0.72
FIELD
VOX1m

Figure 2

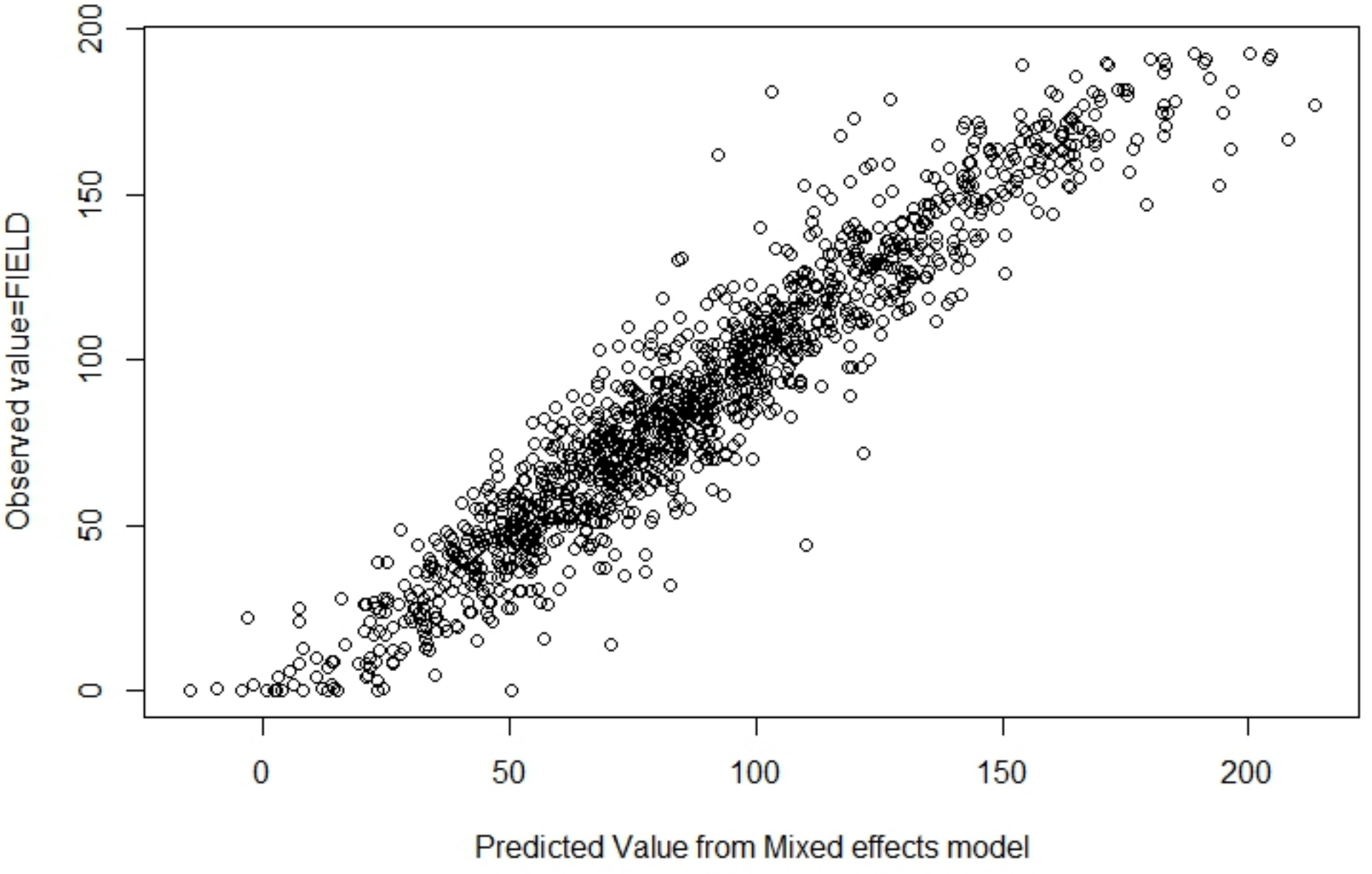
Observed value=FIELD
0
50
100
150
200
Predicted Value from Mixed effects model

Figure 3

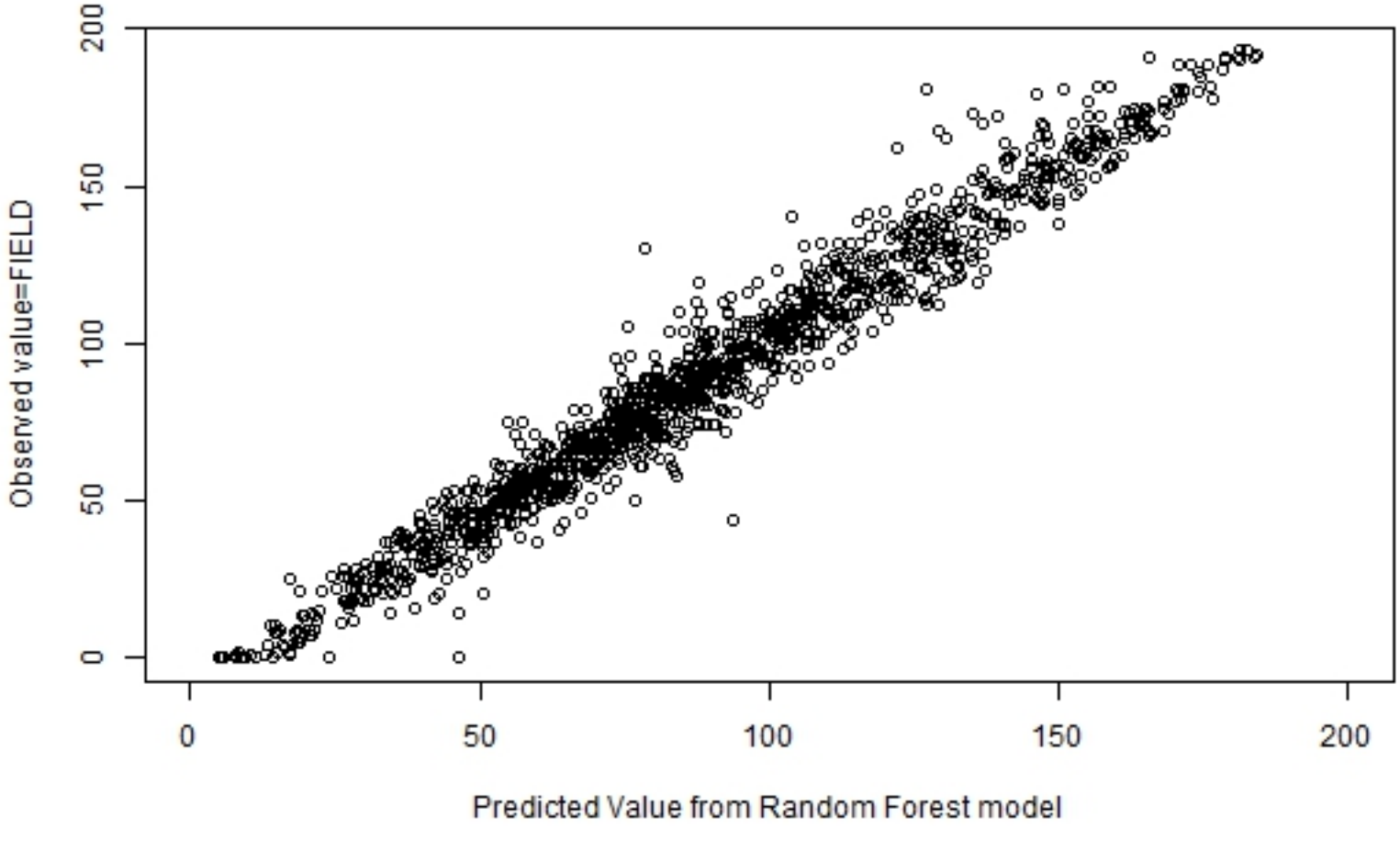
Observed value=FIELD
0
50
100
150
200
Predicted Value from Random Forest model

Figure 5

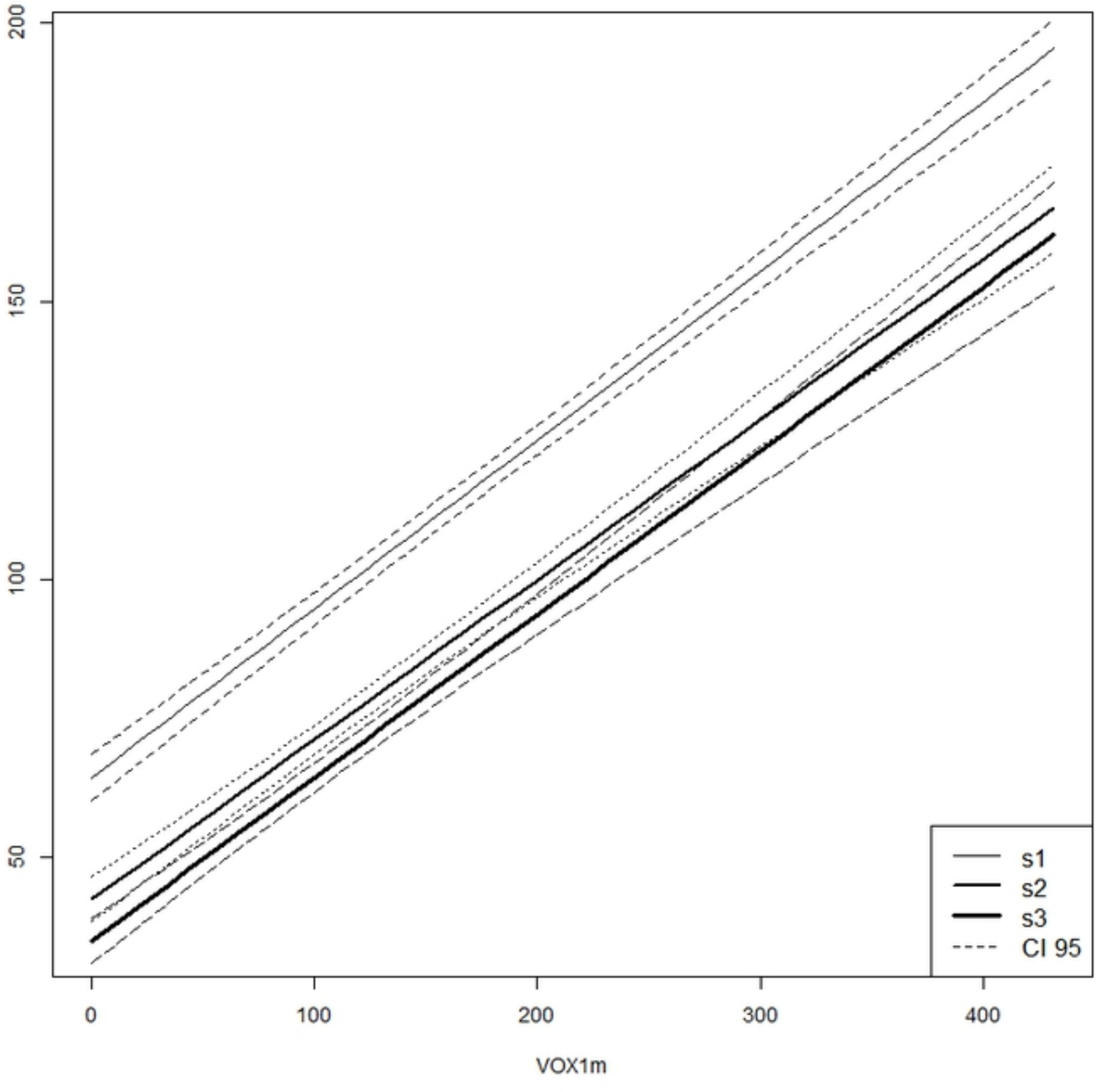

Figure 4